microbial biotechnology

Open Access

Targeting of fluorescent *Lactococcus lactis* to colorectal cancer cells through surface display of tumour-antigen binding proteins

Tina Vida Plavec,[1,2] Ana Mitrović,[1] Milica Perišić Nanut,[1] Borut Štrukelj,[1,2] Janko Kos[1,2] and Aleš Berlec[1,2] iD

[1]Department of Biotechnology, Jožef Stefan Institute, Jamova 39, Ljubljana, Slovenia.
[2]Faculty of Pharmacy, University of Ljubljana, Aškerčeva 7, Ljubljana, Slovenia.

Summary

Development of targeted treatment for colorectal cancer is crucial to avoid side effects. To harness the possibilities offered by microbiome engineering, we prepared safe multifunctional cancer cell-targeting bacteria *Lactococcus lactis*. They displayed, on their surface, binding proteins for cancer-associated transmembrane receptors epithelial cell adhesion molecule (EpCAM) and human epidermal growth factor receptor 2 (HER2) and co-expressed an infrared fluorescent protein for imaging. Binding of engineered *L. lactis* to tumour antigens EpCAM and HER2 was confirmed and characterised *in vitro* using soluble receptors. The proof-of-principle of targeting was demonstrated on human cell lines HEK293, HT-29 and Caco-2 with fluorescent microscopy and flow cytometry. The highest *L. lactis* adhesion was seen for the HEK293 cells with the overexpressed tumour antigens, where colocalisation with their tumour antigens was seen for 39% and 67% of EpCAM-targeting and HER2-targeting bacteria, respectively. On the other hand, no binding was observed to HEK293 cells without tumour antigens, confirming the selectivity of the engineered *L. lactis*. Apart from cell targeting in static conditions, targeting ability of engineered *L. lactis* was also shown in conditions of constant flow of bacterial suspension over the HEK293 cells. Successful targeting by engineered *L. lactis* support the future use of these bacteria in biopharmaceutical delivery for the treatment of colorectal cancer.

Introduction

Colorectal cancer (CRC) is the third most common cancer in men and the second in women. It has poor patient prognosis, and although its overall incidence has been decreasing due to successful screening of patients ≥ 50 years, an increase in incidence has been observed for young adults (Siegel *et al.*, 2017; Vuik *et al.*, 2019).

New treatment approaches involve multifunctional agents, and consider the role of both the immune system and the gut microbiome in CRC development (Darbandi *et al.*, 2019). Probiotics that include lactic acid bacteria (LAB) can modulate the gut microbiome composition towards health-promoting strains, or directly suppress CRC through production of short-chain fatty acids, carcinogen binding, competitive exclusion of pathogens, antioxidant activity, reduction of DNA damage and immunomodulation (Chong, 2014).

The advantages of the use of LAB include their oral administration, which allows for local intestinal delivery and their direct interactions with CRC cells, as well as their survival during passage through the gastrointestinal tract (Cano-Garrido *et al.*, 2015). Additionally, LAB are amenable to genetic engineering which can further improve their intrinsic potential for CRC treatment. The most commonly used genera are *Lactobacillus* and *Lactococcus*. The model LAB organism *Lactococcus lactis* is well-characterised and recognised as a food-grade organism that does not colonize the intestines, allowing for its use as a delivery vector. Various genetic engineering tools and expression systems have been developed for *L. lactis*, and they have enabled the expression of different heterologous proteins (Plavec and Berlec, 2019). The use of engineered *L. lactis* raises safety concerns, but these have also been addressed in several studies (reviewed in Plavec and Berlec, 2020). Administration of engineered *L. lactis* would thus allow targeting, detecting and treating of CRC cells.

Engineered *L. lactis*, as well as other LAB, have been tested as gastro-intestinal tract delivery vehicles

for anti-inflammatory cytokines (interleukin-10; Steidler, 2002; Martín *et al.*, 2014), pro-inflammatory cytokine-binding or chemokine-binding proteins (Kosler *et al.*, 2017; Skrlec *et al.*, 2017; Plavec *et al.*, 2019) and mucosal protective proteins (e.g., Trefoil factor 1; Van-denbroucke *et al.*, 2004), some of which have already been tested in clinical trials. The anticancer applications of engineered *L. lactis* include delivery of the antioxi-dant enzyme catalase (de Moreno de LeBlanc *et al.*, 2008), the angiogenesis inhibitor endostatin (Li and Li, 2005), and the apoptotic peptide kisspeptin (Zhang *et al.*, 2016). We have recently demonstrated lectin-based targeting of carbohydrate tumour-antigens on cancer cells by *L. lactis* (Plavec and Zahirović, 2021). However, to the best of our knowledge, no LAB that target protein tumour-antigens on cancer cells have been reported yet.

Tumour-antigen-specific engineered LAB would recog-nize and attach only to cancer cells. Epithelial cell adhe-sion molecule (EpCAM, CD326; Chaudry *et al.*, 2007; van der Gun *et al.*, 2010; Seeber *et al.*, 2016; Vazquez-Iglesias *et al.*, 2019) and human epidermal growth factor receptor 2 (HER2, CD340; Siena *et al.*, 2018; Gbolahan and O'Neil, 2019; Li *et al.*, 2019) are relevant tumour associated transmembrane glycoprotein receptors in CRC. Their importance has resulted in the development of several high-affinity protein binders, including designed ankyrin repeat proteins (DARPins; Stefan *et al.*, 2011) and affitins against EpCAM (Kalichuk *et al.*, 2018), and affibodies against HER2 (Orlova *et al.*, 2006; Feldwisch *et al.*, 2010). Recently, the potential of tumour-targeted gene knockdown using EpCAM aptamer has been reported for management of aggressive breast cancers (Zhang *et al.*, 2021), while DARPins against HER2 and EpCAM were fused with toxins and combined to effectively prevent the tumour escape (Shramova *et al.*, 2020).

In this study, we engineered the LAB *L. lactis* for sur-face display of protein tumour-antigen targeting pro-teins, and we evaluated the bacterial binding to cancer cells. Two tumour-targeting proteins were applied: an affitin against EpCAM and an affibody against HER2. For concomitant imaging of the bound *L. lactis*, they were also engineered to express infrared fluorescent protein (IRFP) that previously enabled *in vivo* imaging of LAB in mice due to good tissue penetration of infra-red light (Berlec *et al.*, 2015), as well as imaging in cell models of cancer. These engineered *L. lactis* specifi-cally bound to three human cell lines (i.e., HEK293, HT-29, Caco-2 cells) under both static and flow condi-tions. This study thus demonstrates that these multi-functional engineered *L. lactis* can selectively target and visualize these protein tumour antigens on cancer cells.

Results

Expression of EpCAM- and HER2-targeting proteins and their co-expression with IRFP in L. lactis

The genes for the targeting proteins affitin (AffEpCAM; targeting EpCAM), and the affibody (Z-HER; targeting HER2) were fused with the Usp45 secretion signal, with a non-covalent lactococcal surface anchor cAcmA, and optionally with a FLAG-tag for detection. The gene fusion was cloned, together with the gene for IRFP fluo-rescent protein for visualisation, into dual protein expres-sion plasmid pNZDual, similar to previous reports (Berlec *et al.*, 2018; Plavec and Zahirović, 2021). The cloned pNZDual derivatives are listed in Table S1, and the expressed proteins are shown schematically in Fig. 1A.

Expression of the FLAG-labeled targeting proteins AffEpCAM and Z-HER was confirmed in *L. lactis* cell lysates using western blotting (Fig. 1B). Significant sur-face display of the FLAG-labeled targeting proteins on the surface of *L. lactis* was confirmed using flow cytome-try (Fig. 1C), in comparison to the empty plasmid control (pNZ8148), and to *L. lactis* expressing IRFP (plasmid pNZD-IRFP). Dot plots of the flow cytometry data and the gating strategy used to generate Fig. 1C are pre-sented in Fig. S1. An increase in mean fluorescence intensity (MFI) was seen for *L. lactis* that displayed either of the targeting proteins, AffEpCAM or Z-HER (plasmids: pNZDflagEpCAM-IRFP, pNZDflagHER-IRFP respec-tively; Table S1); with the surface display of the HER2 targeting protein demonstrating considerably higher MFI. Concomitant expression of IRFP was also confirmed for both of the recombinant *L. lactis* that displayed the tar-geting proteins, as determined by fluorescence intensity measurements (Fig. 1D) and colocalisation observed with fluorescence microscopy (74.9% for pNZDflagHER-IRFP-containing cells in comparison to 0.2% for pNZD-IRFP control; Fig. 1E). Expression of IRFP when coex-pressed with AffEpCAM and Z-HER surface fusions was lower than when expressed alone, which was in agree-ment with the previous reports (Berlec *et al.*, 2018; Pla-vec and Zahirović, 2021).

Binding of EpCAM- and HER2-targeting L. lactis to recombinant human antigens and determination of affinities

The functionalities of AffEpCAM and Z-HER displayed on the *L. lactis* surface were confirmed by their binding to the recombinant human receptors EpCAM and HER2 fused to the Fc region of human IgG. The use of recep-tor–IgG chimaeras allowed specific detection by flow cytometry. AffEpCAM-displaying *L. lactis* significantly
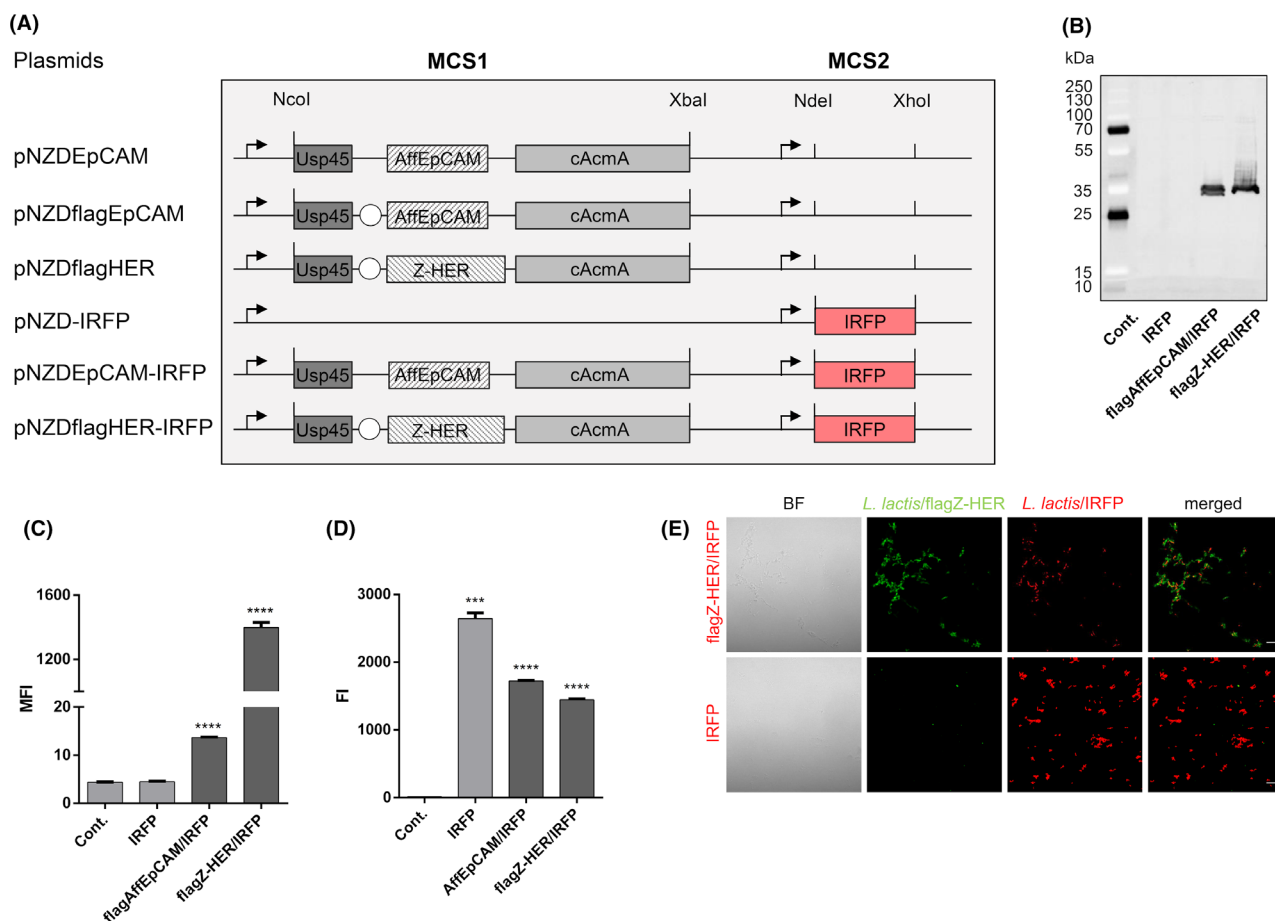
Fig. 1. (A) Scheme of the genetic constructs for surface display of the targeting proteins. Usp45, secretion signal; AffEpCAM, EpCAM-targeting affitin; Z-HER, HER2-targeting affibody; cAcmA, surface anchor; IRFP, infrared fluorescent protein; MCS, multiple cloning site. Arrows indicate nisin promoter. White circles indicate FLAG-tag. (B–E) Co-expression of EpCAM and HER2 tumour-antigen targeting proteins and IRFP in *L. lactis* detected by western blotting of *L. lactis* cell lysates (B), flow cytometry (C), fluorescence intensity measurement (D) and confocal microscopy (for HER2-targeting; E). BF, bright-field channel; *L. lactis*/flagZ-HER, *green fluorescence channel showing FLAG-tagged HER2-targeting affibody; L. lactis*/IRFP, red fluorescence channel showing infrared fluorescent protein. Scale bars, 10 μm. Cont., *L. lactis* containing empty plasmid (pNZ8148); IRFP, *L. lactis* expressing infrared fluorescent protein; AffEpCAM/IRFP, *L. lactis* expressing EpCAM-targeting affitin and IRFP; flagAffEpCAM/IRFP, *L. lactis* expressing FLAG-tagged EpCAM-targeting affitin and IRFP; flagZ-HER/IRFP, *L. lactis* expressing FLAG-tagged HER2-targeting affibody and IRFP; (M)FI, (mean) fluorescence intensity. Data are means ± standard deviation. ***$P < 0.001$, ****$P < 0.0001$ (Student's *t* tests) relative to Cont.

bound recombinant human EpCAM, although this EpCAM binding was considerably lower with the FLAG-tag fused to the targeting protein (i.e., flagAffEpCAM; Fig. S2A); probably due to lower yield of expression (Fig. S3). Therefore, a variant without FLAG-tag (AffEp-CAM) was used for further analysis. Significant binding of FLAG-labeled Z-HER (i.e., flagZ-HER; Fig. S2B) to its recombinant human HER2 target protein was also demonstrated, and removal of FLAG-tag was not needed here. When comparing these two tumour-antigen target-ing proteins, *L. lactis* that displayed Z-HER exhibited higher levels of binding than *L. lactis* that displayed AffEpCAM. Dot plots of the flow cytometry data and the gating strategy used to generate Fig. S2A and B are presented in Figs S4 and S5.

Determination of the affinities of these engineered *L. lactis* (i.e., displaying either AffEpCAM or Z-HER) for their corresponding human receptors (i.e., tumour anti-gens) was also carried out by flow cytometry. Increasing concentrations of the recombinant tumour antigen resulted in increased signals, which corresponded to increased binding to the bacterial surface. The dissocia-tion constant (K_D) was calculated in GraphPad using equation for specific binding with Hill slope (Weiss, 1997). Binding of *L. lactis* that displayed AffEpCAM was characterised by a steep curve with Hill coefficient = 1 (Fig. S2C), suggesting non-cooperative binding. On the contrary, binding of *L. lactis* that displayed Z-HER was characterised by a sigmoidal curve (Fig. S2D) with Hill coefficient > 1, suggesting positive cooperative binding,

possibly due to receptor oligomerisation on the bacterial surface. The calculated values were $K_D = 8.031$ μg ml^{-1} (148 nM; $R^2 = 0.9918$) for the AffEpCAM-displaying *L. lactis*, and $K_D = 1.447$ μg ml^{-1} (14.9 nM; $R^2 = 0.9800$) for the Z-HER-displaying *L. lactis* respectively. These K_D values are approximately three orders of magnitude higher than those reported for isolated EpCAM and HER2 binding proteins, which were in the picomolar range (Orlova *et al.*, 2006; Feldwisch *et al.*, 2010; Kalichuk *et al.*, 2018). However, determined values represent cell population-level parameters and cannot be directly compared to those of isolated proteins (Z-HER/ HER2 or AffEpCAM/EpCAM binding) due to the size of the bacterial cell (in comparison to the tumour antigens), and presence of multiple binders on a single bacterial cell. The K_D values correlated with the amount of protein that was displayed on the *L. lactis* surface, with better surface display of Z-HER (Fig. 1) also resulting in much lower K_D.

Adhesion of EpCAM- and HER2-targeting L. lactis *to HEK293 and cancer cells*

To study adhesion of *L. lactis,* the expression of the tumour antigens EpCAM and HER2 in the HEK293 cells and the HT-29 and Caco-2 CRC cells was confirmed using western blotting and immunocytochemistry. HEK293 cells transfected with the plasmids that encoded EpCAM and HER2 in fusion with fluorescent proteins sfGFP and mEmerald respectively (i.e., EpCAM-sfGFP, HER2-mEm), resulted in overexpression of both of these proteins, as observed by western blot and fluorescence microscopy (Fig. S6A–D). As a control, no expression of EpCAM and HER2 was detected in nontransfected HEK293 cells and HEK293 cells exposed to the transfection reagent without the plasmid (Fig. S6A and B). Immunocytochemical staining further demonstrated EpCAM and HER2 expression in the transfected HEK293 cells, where anti-EpCAM and anti-HER2 antibodies colocalised with respective tumour antigens (Fig. S6C and D). In Caco-2 cells, only EpCAM was detected with western blot (Fig. S6A, band at ∼ 40 kDa), while in HT-29 cells, both EpCAM and HER2 were detected (HER2 as a band at ∼ 200 kDa, Fig. S6B). On the other hand, with immunocytochemical staining, expression of both tumour antigens was observed in the nontransfected HT-29 and Caco-2 cancer cells (Fig. S6E and F).

Lactococcus lactis expressing the EpCAM- or HER2- targeting proteins together with IRFP showed strong adhesion to HEK293 cells transfected for EpCAM and HER2 overexpression, and no adhesion to nontransfected HEK293 cells (Fig. 2A and B). Adhesion of the engineered *L. lactis* to nontransfected HT-29 (Fig. 2C)

and Caco-2 (Fig. 2D) cells was lower than to transfected HEK293, but remained significant compared to the control *L. lactis* that did not adhere to any of the cell types. *Lactococcus lactis* adhesion to these cells was quantified by counting the cell-attached *L. lactis* on micrographs (Fig. 2E–G). Overexpression of the tumour antigens in the transfected HEK293 cells resulted in the greatest *L. lactis* adhesion. Namely, 31 EpCAM-targeting *L. lactis* cells and 50 HER2-targeting *L. lactis* cells adhered per single transfected HEK293 cell (Fig. 2E). The *L. lactis* adhesion to the HT-29 cells was only 0.45 EpCAM- and 0.36 HER2-targeting *L. lactis* cells per single HT-29 cell (Fig. 2F), with higher levels seen for the Caco-2 cells, at 6 and 2, respectively, per single Caco-2 cell (Fig. 2G). For the transfected HEK293 cells, the proportions of the *L. lactis* cells that colocalised with their relevant tumour antigens were also calculated, with colocalisation of 39% for (sfGFP labeled) EpCAM, and colocalisation of 67% for (mEmerald labeled) HER2.

Flow cytometry analysis of adhesion of EpCAM- and HER2-targeting L. lactis *to HEK293 cells*

On the basis of the transfected HEK293 cells showing the highest levels of adhesion under confocal microscopy, these cells were used for imaging flow cytometry assessment of engineered *L. lactis* adhesion. Significant adhesion of both EpCAM- and HER2-targeting *L. lactis* to the transfected HEK293 cells was demonstrated by the greater proportion of double-positive HEK293 cells in the upper right quadrant of the flow cytometry analysis, in comparison to the controls (Fig. 3A and C). Imaging flow cytometry additionally allows visualisation of each cell analysed. Ten images of randomly selected events in the upper right quadrant were inspected for adhesion of *L. lactis* (Fig. S7). Specific adhesion to the HEK293 cells was seen in all of the images for *L. lactis* with the surface-displayed targeting proteins, with no specific adhesion to the HEK293 cells for the control *L. lactis*. The specificity of this *L. lactis* adhesion was further demonstrated by inspection of five images of randomly selected events in the lower right quadrant of the flow cytometry analysis. The absence of *L. lactis* adhesion was confirmed (Fig. S8). Spot count analysis was applied for quantification of the *L. lactis* load per cell, which indicated a mean of seven spots of EpCAM-targeting *L. lactis* per cell, and 11 spots of HER2-targeting *L. lactis* per cell. Lower resolution of imaging flow cytometry in comparison to confocal microscopy limited its applicability to resolve individual cells and perform quantification in Caco-2 and HT-29 cells.

Similar analysis was carried out with standard double-laser flow cytometry. In comparison to the control *L. lactis*, significant adhesion of both EpCAM-targeting
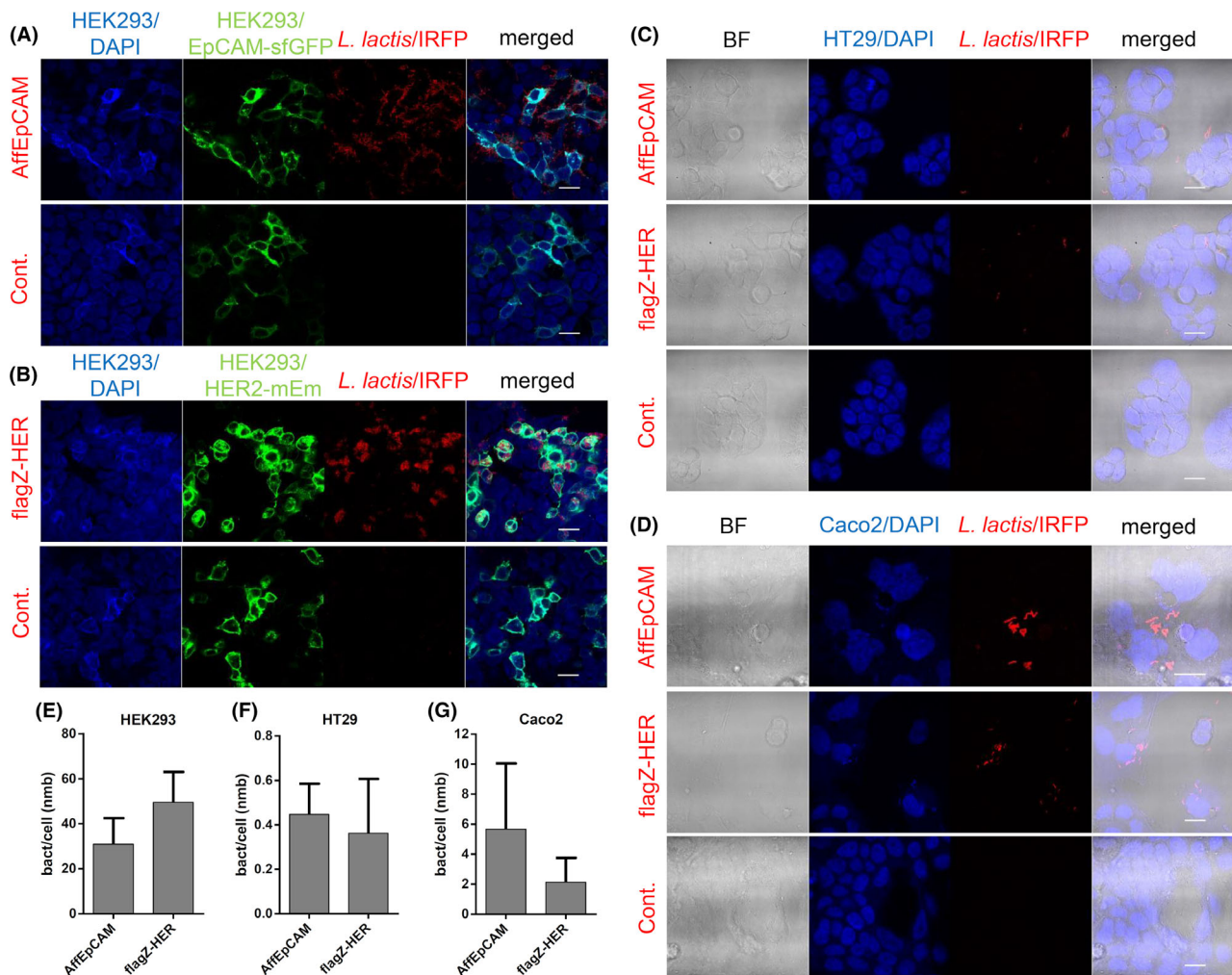
Fig. 2. Representative confocal microscopy images of adhesion of EpCAM-targeting and HER2-targeting *L. lactis* cells to HEK293 cells transfected for EpCAM and HER2 overexpression (A, B) and to nontransfected HT-29 (C) and Caco-2 (D) cancer cells, with quantitative analysis of this adhesion (E–G). AffEpCAM, *L. lactis* displaying AffEpCAM and expressing IRFP; flagZ-HER, *L. lactis* displaying FLAG-labeled Z-HER and expressing IRFP; Cont., *L. lactis* expressing IRFP; DAPI, DAPI channel; HEK293/EpCAM-sfGFP, green fluorescence channel showing HEK293 cells overexpressing sfGFP-labeled EpCAM; HEK293/HER2-mEm, green fluorescence channel showing HEK293 cells overexpressing mEmerald-labeled HER2; *L. lactis*/IRFP, red fluorescence channel showing *L. lactis*; BF, bright-field channel.

(Fig. S9A) and HER2-targeting (Fig. S9B) *L. lactis* to the HEK293 cells was demonstrated. Adhesion of the HER2-targeting *L. lactis* to the HEK293 cells was greater than that of the EpCAM-targeting *L. lactis,* as indicated by the higher proportions (%) of double positive cells in the upper right quadrant.

Real-time imaging of adhesion of EpCAM- and HER2-targeting L. lactis *to HEK293 cells under continuous flow conditions*

To simulate the conditions in the gastrointestinal tract, the real-time adhesion of EpCAM-targeting and HER2-targeting *L. lactis* to the HEK293 cells was also investigated under conditions of continuous flow, over 135 min.

The cultures of *L. lactis* coexpressing AffEpCAM and IRFP or Z-HER and IRFP were individually taken into a syringe and slowly pumped through sterile silicone tubes to the channel slide with the relevant transfected HEK293 cells. The *L. lactis* that coexpressed AffEpCAM and IRFP or Z-HER and IRFP specifically adhered to these human HEK293 cells, as demonstrated by colocalisation of the *L. lactis* cells with EpCAM and HER2 on the HEK293 cells respectively (Fig. 4A, B, E, and F). On the other hand, *L. lactis* expressing IRFP only (the negative controls) did not show adhesion to the HEK293 cells, but rather to the unoccupied parts of the channel slides (Fig. 4C, D, G, and H). On average, 8.5% of the EpCAM-targeting *L. lactis* colocalised with the EpCAM tumour antigen expressed by the HEK293 cells.
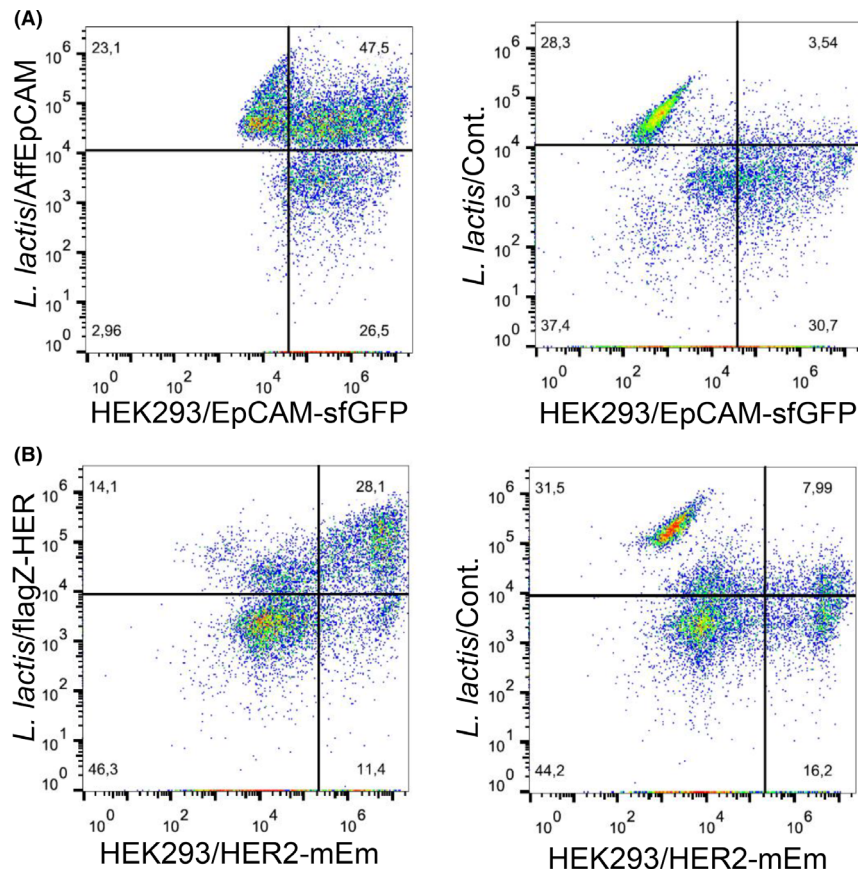
Fig. 3. Imaging flow cytometry analysis of adhesion of EpCAM-targeting (A) and HER2-targeting (B) *L. lactis* to transfected HEK293 cells, in comparison to *L. lactis* expressing IRFP (control bacteria). Scatterplots show the proportions (%) of HEK293 cells in each quadrant. HEK293/EpCAM-sfGFP, HEK293 cells overexpressing sfGFP-labeled EpCAM; HEK293/HER2-mEm, HEK293 cells overexpressing mEmerald-labeled HER2; *L. lactis*/AffEpCAM, *L. lactis* displaying AffEpCAM and expressing IRFP; *L. lactis*/flagZ-HER, *L. lactis* displaying FLAG-labeled Z-HER and expressing IRFP; *L. lactis*/Cont., *L. lactis* expressing IRFP.

However, large amounts of *L. lactis* aggregates were located around the cell edges, which suggests that the proportion of adhered *L. lactis* might be underestimated. Nevertheless, this *L. lactis* adhesion was significant compared to the negative control, where only up to 1% of the *L. lactis* colocalised with EpCAM. On the other hand, 37% of the HER2-targeting *L. lactis* colocalised with the HER2 tumour antigen expressed by the HEK293 cells, while the control *L. lactis* did not show any colocalisation. Therefore, both of these targeting proteins allowed successful adhesion of the *L. lactis* cells, compared to the respective controls. For the kinetics of this *L. lactis* adhesion, those that were HER2 targeting (Fig. 4F) reached higher levels of adhered *L. lactis* sooner than for the EpCAM-targeting *L. lactis* (Fig. 4B).

Discussion

Wild-type and engineered LAB have shown beneficial effects for protection against CRC in several previous studies (de Moreno de LeBlanc *et al.*, 2008; Zhong *et al.*, 2014; Hendler and Zhang, 2018; Eslami *et al.*, 2019). However, the selective targeting of cancer cells is crucial to enhance their beneficial effects and prevent potential side effects. Recently, we used lectin-based targeting of glycan tumour antigens on cancer cells (Plavec and Zahirović, 2021); while in the present study, we displayed two proteins on the surface of the LAB *L. lactis* that bound protein tumour-antigens, and investigated the cancer-cell-targeting of these engineered bacteria. We targeted two transmembrane proteins, EpCAM and HER2 that are known to be overexpressed on the surface of CRC cells, and are recognised as tumour antigens.

Significant levels of expression and surface display on *L. lactis* of EpCAM- and HER2- targeting proteins was confirmed. However, the display of the EpCAM-targeting protein (affitin AffEpCAM) was lower by more than a factor of 100 compared to the display of the HER2-targeting protein (affibody Z-HER). Similarly, AffEpCAM-displaying
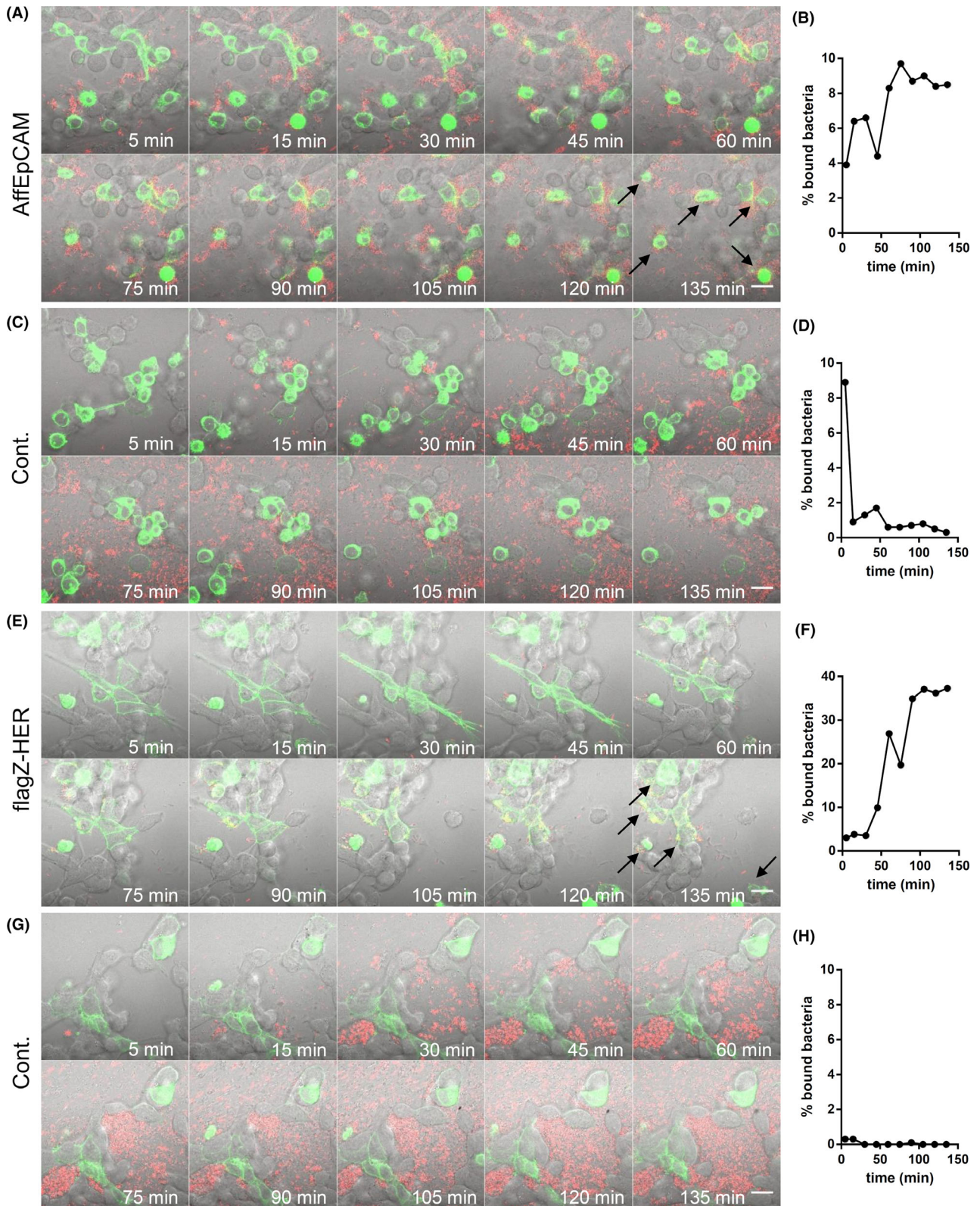
Fig. 4. Representative real-time imaging of adhesion of EpCAM-targeting (A) and HER2-targeting (E) *L. lactis,* in comparison to control *L. lactis* (C, G), to HEK293 overexpressing EpCAM (A, C) or HER2 (E, G). The attachment kinetics are also shown (right), with colocalisation of *L. lactis* and EpCAM (B, D) or HER2 (F, H) as a function of time. Scale bars, 20 μm. AffEpCAM, *L. lactis* displaying AffEpCAM and expressing IRFP; flagZ-HER, *L. lactis* displaying FLAG-labelled Z-HER and expressing IRFP; Cont., *L. lactis* expressing IRFP. Arrows denote regions of colocalisation.

L. lactis showed low binding of the soluble recombinant human EpCAM tumour antigen, which increased by 10-fold after omitting the FLAG-tag, that affected AffEpCAM yield. This was corroborated by dissociation constant (K_D) for the interaction between the engineered *L. lactis* and recombinant tumour antigens that was determined to be in the nanomolar range for both of the *L. lactis* variants (EpCAM-targeting, 148 nM; HER2-targeting 14.9 nM); thereby confirming the considerable affinity of the engineered *L. lactis* for these tumour antigens. IRFP, enabling *in vivo* imaging on mouse model (Berlec *et al.*, 2015), was coexpressed with both of the targeting proteins, AffEpCAM and Z-HER, similar to previous reports (Berlec *et al.*, 2018; Plavec and Zahirović, 2021).

Expression of EpCAM and HER2 tumour antigens in the nontransfected HT-29 and Caco-2 cells was lower than that in the transfected HEK293 cells, where overexpression was driven by the strong promoters. Comparable expression of EpCAM in HT-29 and Caco-2 cells has already been reported using immunofluorescence analysis (Vazquez-Iglesias *et al.*, 2019). Moreover, high expression levels of EpCAM have been seen in both the HT-29 and Caco-2 cells by qPCR (Heine *et al.*, 2012) and flow cytometry (Vallera *et al.*, 2013). Here, we also observed similar expression of HER2 in the HT-29 and Caco-2 cells by both western blotting and immunofluorescence analysis.

The adhesion of engineered *L. lactis* to the human cells depended on the cell lines. According to expectation, the highest *L. lactis* adhesion was seen, by confocal microscopy, for the transfected HEK293 cells with the overexpressed tumour antigens, with 31 EpCAM-targeting and 50 HER2-targeting *L. lactis* cells per HEK293 cell. The attachment to the wild-type CRC cells was lower: for the Caco-2 cells for approximately the factor of ten, and for the HT-29 cells for the factor of 100. Nevertheless, in comparison to the control *L. lactis*, for which no binding was observed, the significant targeting of the engineered *L. lactis* to these CRC cancer cells was confirmed. Specificity of bacterial binding to only those cells that expressed tumour antigens was also demonstrated. Engineered *L. lactis* adhered to transfected HEK293 cells only, whereas no binding to non-transfected HEK293 cells could be detected by visual inspection.

The adhesion of the EpCAM- and HER2-targeting *L. lactis* to the HEK293 cells, that showed the highest expression of the tumour antigens, was further confirmed using flow cytometry and imaging flow cytometry. For the imaging flow cytometry, the HER2 targeting of *L. lactis* showed 11 spots (corresponding to *L. lactis* cells) per HEK293 cell, and EpCAM targeting seven spots per HEK293 cell; probably due to lower resolving ability of imaging flow cytometry. Nevertheless, the ratio between

EpCAM- and HER2-based targeting was in agreement with the data from flow cytometry and confocal microscopy; thereby suggesting more effective targeting of HER2-binding *L. lactis* to the (HER2-overexpressing) HEK293 cells. This is also in agreement with the 10-fold higher affinity of HER2-targeting *L. lactis* for its respective soluble receptor, and the higher display of the HER2-targeting protein Z-HER on *L. lactis*.

On the contrary, the EpCAM-targeting *L. lactis* adhered more effectively than the HER2-targeting *L. lactis* to the CRC HT-29 and Caco-2 cells. This might be due to greater expression of the EpCAM tumour antigen in these cells, compared to HER2; however, this cannot be directly compared in this study due to the use of different antibodies. It was previously reported that in CRC EpCAM expression was up-regulated by 100-fold to 1000-fold (Seeber *et al.*, 2016), while HER2 expression was up-regulated by fivefold (Owen *et al.*, 2018) and 12-fold (Blok *et al.*, 2013). Nevertheless, HER2 overexpression has been shown in patients with CRC (Ross and McKenna, 2001), and it has been suggested as a promising alternative therapeutic target (Ingold Heppner *et al.*, 2014; Greally *et al.*, 2018; Ross *et al.*, 2018).

Studies of bacteria adhesion to cultured cells typically conducted statically in microtiter plates (Acord *et al.*, 2005; Chen *et al.*, 2017; Garcia-Gonzalez *et al.*, 2018; Plavec and Zahirović, 2021) come with inherent drawbacks. The conditions in microtiter plates do not resemble physiologic conditions in the gastrointestinal tract, in which the bacteria and cells encounter each other under constant flow. Assays in flow devices allow observation of dynamic events in real time such as bacterial attachment and adhesion, and they introduce the flow of the physiologically relevant fluid. Moreover, live-imaging assays provide control of the liquid shear stress, as well as constant monitoring of the adhesion process (Staerk *et al.*, 2016; Pedersen *et al.*, 2018).

Here, we studied the adhesion of tumour-antigen targeting *L. lactis* cells to live human HEK293 cells under constant flow in fluidic device over > 2 h. This system supported the data obtained here for the microtiter plate format, and showed significant and specific targeting of the engineered *L. lactis* to the HEK293 cells in a time-dependent manner. The engineered *L. lactis* showed adhesion to only the transfected HEK293 cells that expressed the relevant target, EpCAM or HER2, and no adhesion was seen to the nontransfected HEK293 cells. For the adhesion kinetics, HER2-targeting *L. lactis* adhered to HEK293 cells faster than EpCAM-targeting *L. lactis*, which might be the consequence of the lower K_D that we determined *in vitro*. Additionally, compared to EpCAM-targeting bacteria, larger levels (fourfold) of HER2-targeting bacteria adhered to the HEK293 cells over the time period. These data indicate that the

engineered HER2-binding *L. lactis* developed in this study shows superior adhesion to the EpCAM-binding *L. lactis*. However, the EpCAM-binding *L. lactis* would probably be more clinically relevant for targeting CRC cells and tumours. To further improve EpCAM targeting, novel EpCAM-directed non-immunoglobulin scaffolds could be applied or developed, or an increase in the level of surface display could be attempted. Additionally, combination of EpCAM and HER2 targeting should be tested for possible synergy, as reported recently for effective toxin delivery (Shramova *et al.*, 2020).

Conclusion

We have shown specific binding of *L. lactis* with surface-displayed EpCAM-targeting and HER2-targeting proteins to their respective tumour antigens on human cells in static conditions and in constant flow. This system is a step toward bacteria-based CRC theranostics.

Experimental procedures

Bacterial strains, media and growth conditions

The bacterial strains used in this study are listed in Table S1. *Escherichia coli* strain DH5α was grown with aeration at 37°C, in lysogeny broth medium supplemented with ampicillin (100 μg ml^{-1}). *Lactococcus lactis* NZ9000 was grown without aeration at 30°C, in M-17 medium (MilliporeSigma, Burlington, MA, USA) supplemented with 0.5% glucose (GM-17) and chloramphenicol (10 μg ml^{-1}). Biliverdin HCl (15.5 μg ml^{-1}; Sigma Aldrich, St. Louis, MO, USA) was added for expression of IRFP.

Molecular cloning

The detailed protocol is provided in Supplementary Experimental procedures.

Expression of targeting proteins in L. lactis

The detailed protocol is provided in Supplementary Experimental procedures.

Fluorescence of IRFP

The detailed protocol is provided in Supplementary Experimental procedures.

Human cell cultures

The HEK293 (ATCC CRL-1573) and Caco-2 (ATCC HTB-37) human cell lines were cultured and passaged in Dulbecco's modified Eagle's medium with GlutaMAX™

supplement (Gibco, Thermo Fisher Scientific, Waltham, MA, USA), and the HT-29 human cell line (ATCC HTB-38) in McCoy's 5A Modified Medium (ATCC), each supplemented with 10% (v/v) foetal bovine serum (Gibco) and 1% penicillin-streptomycin (Gibco; corresponding to 100 U/ml penicillin, 100 μg ml^{-1} streptomycin). For Caco-2 cell culturing, 25 mM HEPES (Gibco) and 1% minimum essential medium non-essential amino acids solution (Gibco) were added. All cell lines were incubated, maintained, and cultured at 37°C with 5% CO$_2$. All cell lines had tested negative for mycoplasma (Mycoplasmacheck, Eurofins Genomics, Ebersberg, Germany). Unless otherwise stated, the cells were seeded into 24-well tissue culture plates (Corning, Thermo Fisher Scientific).

HEK293 cell transfection

The detailed protocol is provided in Supplementary Experimental procedures.

SDS-PAGE and western blotting

The detailed protocol is provided in Supplementary Experimental procedures.

Flow cytometry analysis of targeting proteins displayed on the surface of L. lactis

For determination of binding affinity, 20 μl bacteria cultures expressing AffEpCAM/IRFP was added to 500 μl phosphate-buffered saline (PBS) and centrifuged at 5000 g for 5 min at 4°C. The pellets were resuspended in 250 μl PBS containing increasing concentrations of recombinant human EpCAM/TROP-1 Fc chimaera (0.0, 0.05, 0.1, 0.25, 0.5, 1.0, 1.5, 2.0, 3.0, 4.0 μg ml^{-1}). Similarly, 20 μl bacteria culture expressing flagZ-HER/IRFP in the stationary phase was added to 500 μl PBS containing increasing concentrations of recombinant human ErbB2/Her2 Fc chimaera (0.0, 0.05, 0.1, 0.25, 0.5, 0.75, 1.0, 1.5, 2.0, 3.0 μg ml^{-1}). After 2 h of incubation at room temperature with constant shaking at 100 rpm, the cells were washed three times with 200 μl 0.1% PBST, and resuspended in 250 μl PBS containing Alexa Fluor 488 anti-human Fcγ specific antibody (1:1000; Jackson ImmunoResearch, West Grove, PA, USA). After 2 h of incubation at room temperature with constant shaking at 100 rpm, the cells were washed three times with 200 μl 0.1% PBST, and finally resuspended in 500 μl PBS.

All samples were analysed using a flow cytometer (FACS Calibur; BD Biosciences, Franklin Lakes, NJ, USA) at excitation 488 nm and emission 530 nm in the FL1 channel. The geometric MFI of at least 20 000 bacterial cells was measured with the appropriate gate. The

means of at least three independent experiments were included.

To calculate the affinity between bacteria and recombinant receptor, nonlinear regression analysis was performed using the GraphPad Prism 6 software (GraphPad Software, San Diego, CA, USA). The equation for specific binding with Hill slope was applied. The values of the control (IRFP-expressing bacteria) were subtracted to analyse only the specific binding. K_D values were converted to molar concentrations.

The complete protocol is provided in Supplementary Experimental procedures.

Fluorescent immunocytochemical staining of EpCAM and HER2

The detailed protocol is provided in Supplementary Experimental procedures.

Adhesion of engineered L. lactis *to human cells*

Adhesion assay was based on the protocol reported in Plavec and Zahirović (2021). The HEK293, HT-29 and Caco-2 human cell lines were seeded into 24-well plates. The seeding concentration was determined for each cell line so as to reach the desired confluence (HEK293 cells: 2×10^5 cells/well; HT-29 cells: 1×10^5 cells/well; Caco-2 cells: 1.5×10^5 cells/well). After 48 h, the medium in the wells was aspirated and 500 µl *L. lactis* cultures (A_{600} 0.8) containing AffEpCAM/IRFP or flagZ-HER/IRFP (diluted in pre-warmed RPMI) were added to each well, for 2 h at 37°C. After this incubation, the wells were gently washed twice with PBS to remove unattached *L. lactis*, and prepared for further microscopy or flow cytometry analysis. For confocal microscopy, sterilised coverslips (diameter, 8 mm; thickness, #1.5) were added to wells before seeding, and the cells were fixed in 4% paraformaldehyde in PBS for 20 min at room temperature, washed twice with PBS, and mounted with DAPI (4',6-diamidino-2-phenylindole)-containing mounting agent. For flow cytometry, the cells with adhered *L. lactis* were transferred to tubes, fixed with 4% paraformaldehyde in PBS for 20 min at room temperature, washed twice with PBS, and finally resuspended in 100 µl PBS.

Confocal microscopy

The detailed protocol is provided in Supplementary Experimental procedures.

Quantification of L. lactis *adhesion to human cells*

The adhesion of *L. lactis* cells to the HEK293, HT-29 and Caco-2 human cells was quantified using the ImageJ software, by counting the number of *L. lactis* in five representative microscopy images taken using the 63× objective lens. The results are expressed as mean numbers of *L. lactis* per human cell ± standard deviation. Human cells were counted using a cell counter plugin for ImageJ (https://imagej.nih.gov/ij/plugins/cell-counter.html), where the cells on the edges were excluded. *Lactococcus lactis* cells were counted using the particle analysis function, with the threshold set manually by visual inspection of the images. The reliability of the method was confirmed by comparing it to manual counting of the adhered *L. lactis*. Linear regression was carried out to validate the accuracy (reliability) of the quantitative analysis method (Lepanto *et al.*, 2014), where R^2 revealed high fits for both sets of data (Fig. S10), supporting the appropriateness of the method.

Quantitative assessment of the proportions (%) of bacteria colocalizing with the tumour antigen EpCAM or HER2 of transfected HEK293 cells was carried out using the ImageJ software with the just another colocalisation program (JaCoP) plugin (https://imagej.nih.gov/ij/plugins/track/jacop.html). We determined the threshold and calculated the Manders' coefficients, to determine the fraction of red pixels in the image (bacteria) that overlapped with green pixels in the image (EpCAM or HER2). Mean data are presented.

The complete protocol is provided in Supplementary Experimental procedures.

Flow cytometric analysis of L. lactis *adhesion to human cells*

Human cells with adhered *L. lactis* were filtered through a 70-µm cell strainer (Corning) prior to loading and analysis. The samples were analysed using a flow cytometer (S3e Sorter; Bio-Rad) at excitation wavelengths 488 and 640 nm. In all, 10 000 events were measured. The FlowJo software was used for data analysis.

Imaging flow cytometric analysis of L. lactis *adhesion to human cells*

Human cells with adhered *L. lactis* were analysed using an imaging flow cytometer (Amnis, Luminex Corporation, Austin, TX, USA). The samples were run at the low-speed setting (~400 cells/s) at excitation wavelengths 488 and 642 nm. The 60× objective was used for the imaging. In all, 10 000 events were measured. The data were analysed using the ImageStream data analysis and exploration software (IDEAS).

Binding of *L. lactis* to the human cells was observed visually as a pattern of bright discrete spots, with little diffuse staining. To quantify the red fluorescent spots on

a cell (corresponding to IRFP-expressing *L. lactis* bound to the cell), spot (M11_IRFP, bright. 6) and peak (M11_IRFP, bright. 4) masks were created in the reference channel for the bacteria. The same masks were applied for both *L. lactis* variants, targeting EpCAM and HER2. The spot mask was used to delineate the *L. lactis* cells, and the peak mask was used to separate the connected spots, although aggregates and overlapping cells could not be completely resolved. Visual validation of mask design was performed to check the accuracy of the selected masks. For the final analysis, the data were exported to the FlowJo software.

Live imaging of bacteria binding to cell cultures

HEK293 cells were transfected with Emerald-ERBB2-N-18 or pcDNA3-EpFL-sfGFP (Gaber *et al.*, 2018), and 24 h post-transfection, 150 μL transfected cells (at 1.6×10^6 cells/ml) were seeded into channel slides (I Luer ibiTreat μ-slides; tissue-culture-treated sterilised coverslips, 0.6 mm; ibidi GmbH, Martinsried, Germany) according to the manufacturer instructions, and left for another 24 h to attach and obtain their characteristic morphological shape. The cultures of *L. lactis* (A_{600} 0.8) expressing AffEpCAM/IRFP or flagZ-HER/IRFP were taken into a syringe, that was inserted into the pump system (DUAL-NE-1000X; New Era Pump Systems, Farmingdale, NY, USA) and connected to a channel slide using sterile silicone tubes. A constant flow rate of 100 μl min^{-1} of bacteria culture was applied for ~2 h at 37°C under 5% CO_2. The conditions were maintained using a stage top incubator (Tokai Hit, Fujinomiya-shi, Shizuoka-ken). A representative microscopy field was chosen and examined. The images were collected after 5 and 15 min, and then after every 15 min, up to 135 min, using a 63× immersion oil objective with settings to detect bright-field, DAPI, Alexa 488, and Alexa 647.

Statistical analyses

Statistical analyses were performed using the GraphPad Prism 6 software. Student's *t* tests were used to define the significances of the differences between the bacteria with tumour-antigen targeting proteins and their respective controls.

Acknowledgements

Conflict of interest

The authors declare no conflicts of interest.

References

Acord, J., Maskell, J., and Sefton, A. (2005) A rapid microplate method for quantifying inhibition of bacterial adhesion to eukaryotic cells. *J Microbiol Methods* **60:** 55–62.

Berlec, A., Skrlec, K., Kocjan, J., Olenic, M., and Strukelj, B. (2018) Single plasmid systems for inducible dual protein expression and for CRISPR-Cas9/CRISPRi gene regulation in lactic acid bacterium *Lactococcus lactis*. *Sci Rep* **8:** 1009.

Berlec, A., Zavrsnik, J., Butinar, M., Turk, B., and Strukelj, B. (2015) In vivo imaging of *Lactococcus lactis*, *Lactobacillus plantarum* and *Escherichia coli* expressing infrared fluorescent protein in mice. *Microb Cell Fact* **14:** 181.

Blok, E.J., Kuppen, P.J., van Leeuwen, J.E., and Sier, C.F. (2013) Cytoplasmic overexpression of HER2: a key factor in colorectal cancer. *Clin Med Insights Oncol* **7:** 41–51.

Cano-Garrido, O., Seras-Franzoso, J., and Garcia-Fruitos, E. (2015) Lactic acid bacteria: reviewing the potential of a promising delivery live vector for biomedical purposes. *Microb Cell Fact* **14:** 137.

Chaudry, M.A., Sales, K., Ruf, P., Lindhofer, H., and Winslet, M.C. (2007) EpCAM an immunotherapeutic target for gastrointestinal malignancy: current experience and future challenges. *Br J Cancer* **96:** 1013–1019.

Chen, Z.Y., Hsieh, Y.M., Huang, C.C., and Tsai, C.C. (2017) Inhibitory effects of probiotic *Lactobacillus* on the growth of human colonic carcinoma cell line HT-29. *Molecules* **22:** 107.

Chong, E.S. (2014) A potential role of probiotics in colorectal cancer prevention: review of possible mechanisms of action. *World J Microbiol Biotechnol* **30:** 351–374.

Darbandi, A., Mirshekar, M., Shariati, A., Moghadam, M.T., Lohrasbi, V., Asadolahi, P., and Talebi, M. (2019) The effects of probiotics on reducing the colorectal cancer surgery complications: a periodic review during 2007–2017. *Clin Nutr* **39:** 2358–2367.

Eslami, M., Yousefi, B., Kokhaei, P., Hemati, M., Nejad, Z.R., Arabkari, V., and Namdar, A. (2019) Importance of probiotics in the prevention and treatment of colorectal cancer. *J Cell Physiol* **234:** 17127–17143.

Feldwisch, J., Tolmachev, V., Lendel, C., Herne, N., Sjöberg, A., Larsson, B., *et al.* (2010) Design of an optimized scaffold for affibody molecules. *J Mol Biol* **398:** 232–247.

Gaber, A., Kim, S.J., Kaake, R.M., Benčina, M., Krogan, N., Šali, A., *et al.* (2018) EpCAM homo-oligomerization is not the basis for its role in cell-cell adhesion. *Sci Rep* **8:** 13269.

Garcia-Gonzalez, N., Prete, R., Battista, N., and Corsetti, A. (2018) Adhesion properties of food-associated *Lactobacillus plantarum* strains on human intestinal epithelial cells and modulation of IL-8 release. *Front Microbiol* **9:** 2392.

Gbolahan, O., and O'Neil, B. (2019) Update on systemic therapy for colorectal cancer: biologics take sides. *Transl Gastroenterol Hepatol* **4:** 9.

Greally, M., Kelly, C.M., and Cercek, A. (2018) HER2: An emerging target in colorectal cancer. *Curr Probl Cancer* **42:** 560–571.

van der Gun, B.T., Melchers, L.J., Ruiters, M.H., de Leij, L.F., McLaughlin, P.M., and Rots, M.G. (2010) EpCAM in carcinogenesis: the good, the bad or the ugly. *Carcinogenesis* **31:** 1913–1921.

Heine, M., Freund, B., Nielsen, P., Jung, C., Reimer, R., Hohenberg, H., *et al.* (2012) High interstitial fluid pressure is associated with low tumour penetration of diagnostic monoclonal antibodies applied for molecular imaging purposes. *PLoS One* **7:** e36258.

Hendler, R., and Zhang, Y. (2018) Probiotics in the treatment of colorectal cancer. *Medicines* **5:** 101.

Ingold Heppner, B., Behrens, H.M., Balschun, K., Haag, J., Kruger, S., Becker, T., and Rocken, C. (2014) HER2/neu testing in primary colorectal carcinoma. *Br J Cancer* **111:** 1977–1984.

Kalichuk, V., Renodon-Cornière, A., Béhar, G., Carrión, F., Obal, G., Maillasson, M., *et al.* (2018) A novel, smaller scaffold for affitins: showcase with binders specific for EpCAM. *Biotechnol Bioeng* **115:** 290–299.

Kosler, S., Strukelj, B., and Berlec, A. (2017) Lactic acid bacteria with concomitant IL-17, IL-23 and TNFalpha-binding ability for the treatment of inflammatory bowel disease. *Curr Pharm Biotechnol* **18:** 318–326.

Lepanto, P., Lecumberry, F., Rossello, J., and Kierbel, A. (2014) A confocal microscopy image analysis method to measure adhesion and internalization of *Pseudomonas aeruginosa* multicellular structures into epithelial cells. *Mol Cell Probes* **28:** 1–5.

Li, J.-L., Lin, S.-H., Chen, H.-Q., Liang, L.-S., Mo, X.-W., Lai, H., *et al.* (2019) Clinical significance of HER2 and EGFR expression in colorectal cancer patients with ovarian metastasis. *BMC Clin Pathol* **19:** 3.

Li, W., and Li, C.B. (2005) Effect of oral *Lactococcus lactis* containing endostatin on 1, 2-dimethylhydrazine-induced colon tumor in rats. *World J Gastroenterol* **11:** 7242–7247.

Martín, R., Chain, F., Miquel, S., Natividad, J.M., Sokol, H., Verdu, E.F., *et al.* (2014) Effects in the use of a genetically engineered strain of *Lactococcus lactis* delivering in situ IL-10 as a therapy to treat low-grade colon inflammation. *Hum Vaccin Immunother* **10:** 1611–1621.

de Moreno de LeBlanc, A., LeBlanc, J.G., Perdigón, G., Miyoshi, A., Langella, P., Azevedo, V., and Sesma, F. (2008) Oral administration of a catalase-producing *Lactococcus lactis* can prevent a chemically induced colon cancer in mice. *J Med Microbiol* **57:** 100–105.

Orlova, A., Magnusson, M., Eriksson, T.L.J., Nilsson, M., Larsson, B., Höidén-Guthenberg, I., *et al.* (2006) Tumor imaging using a picomolar affinity HER2 binding affibody molecule. *Cancer Res* **66:** 4339–4348.

Owen, D.R., Wong, H.L., Bonakdar, M., Jones, M., Hughes, C.S., Morin, G.B., *et al.* (2018) Molecular characterization of ERBB2-amplified colorectal cancer identifies potential mechanisms of resistance to targeted therapies: a report of two instructive cases. *Cold Spring Harb Mol Case Stud* **4:** a002535.

Pedersen, R.M., Grønnemose, R.B., Stærk, K., Asferg, C.A., Andersen, T.B., Kolmos, H.J., *et al.* (2018) A method for quantification of epithelium colonization capacity by pathogenic bacteria. *Front Cell Infect Microbiol* **8:** 16.

Plavec, T.V., and Berlec, A. (2019) Engineering of lactic acid bacteria for delivery of therapeutic proteins and peptides. *Appl Microbiol Biotechnol* **103:** 2053–2066.

Plavec, T.V., and Berlec, A. (2020) Safety aspects of genetically modified lactic acid bacteria. *Microorganisms* **8:** 297.

Plavec, T.V., Kuchar, M., Benko, A., Liskova, V., Cerny, J., Berlec, A., and Maly, P. (2019) Engineered *Lactococcus lactis* secreting IL-23 receptor-targeted REX protein blockers for modulation of IL-23/Th17-mediated inflammation. *Microorganisms* **7:** 152.

Plavec, T.V., and Zahirović, A. (2021) Lectin-mediated binding of engineered *Lactococcus lactis* to cancer cells. *Microorganisms* **9:** 223.

Ross, J.S., Fakih, M., Ali, S.M., Elvin, J.A., Schrock, A.B., Suh, J., *et al.* (2018) Targeting HER2 in colorectal cancer: The landscape of amplification and short variant mutations in ERBB2 and ERBB3. *Cancer* **124:** 1358–1373.

Ross, J.S., and McKenna, B.J. (2001) The HER-2/neu oncogene in tumors of the gastrointestinal tract. *Cancer Invest* **19:** 554–568.

Seeber, A., Untergasser, G., Spizzo, G., Terracciano, L., Lugli, A., Kasal, A., *et al.* (2016) Predominant expression of truncated EpCAM is associated with a more aggressive phenotype and predicts poor overall survival in colorectal cancer. *Int J Cancer* **139:** 657–663.

Shramova, E., Proshkina, G., Shipunova, V., Ryabova, A., Kamyshinsky, R., Konevega, A., *et al.* (2020) Dual targeting of cancer cells with DARPin-based toxins for overcoming tumor escape. *Cancers* **12:** 3014.

Siegel, R.L., Fedewa, S.A., Anderson, W.F., Miller, K.D., Ma, J., Rosenberg, P.S., and Jemal, A. (2017) Colorectal cancer incidence patterns in the United States, 1974–2013. *J Natl Cancer Inst* **109:** 1974–2013.

Siena, S., Sartore-Bianchi, A., Marsoni, S., Hurwitz, H.i., McCall, S.j., Penault-Llorca, F., *et al.* (2018) Targeting the human epidermal growth factor receptor 2 (HER2) oncogene in colorectal cancer. *Ann Oncol* **29:** 1108–1119.

Skrlec, K., Pucer Janez, A., Rogelj, B., Strukelj, B., and Berlec, A. (2017) Evasin-displaying lactic acid bacteria bind different chemokines and neutralize CXCL8 production in Caco-2 cells. *Microb Biotechnol* **10:** 1732–1743.

Staerk, K., Khandige, S., Kolmos, H.J., Moller-Jensen, J., and Andersen, T.E. (2016) Uropathogenic *Escherichia coli* express type 1 fimbriae only in surface adherent populations under physiological growth conditions. *J Infect Dis* **213:** 386–394.

Stefan, N., Martin-Killias, P., Wyss-Stoeckle, S., Honegger, A., Zangemeister-Wittke, U., and Pluckthun, A. (2011) DARPins recognizing the tumor-associated antigen EpCAM selected by phage and ribosome display and engineered for multivalency. *J Mol Biol* **413:** 826–843.

Steidler, L. (2002) *In situ* delivery of cytokines by genetically engineered *Lactococcus lactis*. *Antonie Van Leeuwenhoek* **82:** 323–331.

Vallera, D.A., Zhang, B., Gleason, M.K., Oh, S., Weiner, L.M., Kaufman, D.S., *et al.* (2013) Heterodimeric bispecific

single-chain variable-fragment antibodies against EpCAM and CD16 induce effective antibody-dependent cellular cytotoxicity against human carcinoma cells. *Cancer Biother Radiopharm* **28**: 274–282.

Vandenbroucke, K., Hans, W., Van Huysse, J., Neirynck, S., Demetter, P., Remaut, E., *et al.* (2004) Active delivery of trefoil factors by genetically modified *Lactococcus lactis* prevents and heals acute colitis in mice. *Gastroenterology* **127**: 502–513.

Vazquez-Iglesias, L., Barcia-Castro, L., Rodriguez-Quiroga, M., Paez de la Cadena, M., Rodriguez-Berrocal, J., and Cordero, O.J. (2019) Surface expression marker profile in colon cancer cell lines and sphere-derived cells suggests complexity in CD26(+) cancer stem cells subsets. *Biol Open* **8**: bio041673.

Vuik, F.E.R., Nieuwenburg, S.A.V., Bardou, M., Lansdorp-Vogelaar, I., Dinis-Ribeiro, M., Bento, M.J., *et al.* (2019) Increasing incidence of colorectal cancer in young adults in Europe over the last 25 years. *Gut* **68**: 1820–1826.

Weiss, J.N. (1997) The Hill equation revisited: uses and misuses. *FASEB J* **11**: 835–841.

Zhang, B., Li, A., Zuo, F., Yu, R., Zeng, Z., Ma, H., and Chen, S. (2016) Recombinant *Lactococcus lactis* NZ9000 secretes a bioactive kisspeptin that inhibits proliferation and migration of human colon carcinoma HT-29 cells. *Microb Cell Fact* **15**: 102.

Zhang, Y., Xie, X., Yeganeh, P.N., Lee, D.-J., Valle-Garcia, D., Meza-Sosa, K.F., *et al.* (2021) Immunotherapy for breast cancer using EpCAM aptamer tumor-targeted gene knockdown. *PNAS* **118**: e2022830118.

Zhong, L., Zhang, X., and Covasa, M. (2014) Emerging roles of lactic acid bacteria in protection against colorectal cancer. *World J Gastroenterol* **20**: 7878–7886.

Supporting information

Additional supporting information may be found online in the Supporting Information section at the end of the article.

Table S1. Strains, primers, plasmids and synthetic genes used in this study.

Table S2. Cell lines and their characteristics.

Fig. S1. (A–D) Flow cytometry analysis of co-expression of EpCAM (C) and HER2 (D) tumor-antigen targeting proteins and IRFP in *L. lactis*, presented by the dot plot display mode of forward scatter (FCS) versus side scatter (SSC). (E–I) Flow cytometry analysis of co-expression of EpCAM (G) and HER2 (H) tumor-antigen targeting proteins and IRFP in *L. lactis*, presented by fluorescence measured in channel FL1. (J) The display of the targeting protein as a shift of the bacteria along the FL1 axis, presented by histogram. Cont., *L. lactis* containing empty plasmid (pNZ8148); IRFP, *L. lactis* expressing infrared fluorescent protein; flagAffEpCAM/IRFP, *L. lactis* expressing FLAG-tagged EpCAM-targeting affitin and IRFP; flagZ-HER/IRFP, *L. lactis* expressing FLAG-tagged HER2-targeting affibody and IRFP.

Fig. S2. (A, B) Flow cytometric confirmation of binding of the *L. lactis* displaying the targeting proteins AffEpCAM (A) and Z-HER (B) to their respective tumor antigens (EpCAM, HER2). (C, D) Determination of the binding affinities of the *L. lactis* displaying the targeting proteins AffEpCAM (C) and Z-HER (D) for their respective tumor antigens. Cont., *L. lactis* containing empty plasmid (pNZ8148); IRFP, *L. lactis* expressing infrared fluorescent protein; AffEpCAM/IRFP, *L. lactis* expressing EpCAM-targeting affitin and IRFP; flagAffEpCAM/IRFP, *L. lactis* expressing FLAG-tagged EpCAM-targeting affitin and IRFP; flagZ-HER/IRFP, *L. lactis* expressing FLAG-tagged HER2-targeting affibody and IRFP; (M)FI, (mean) fluorescence intensity. Data are means ± standard deviation. **$P < 0.01$, ****$P < 0.0001$ (Student's *t* tests) relative to Cont.

Fig. S3. Coommassie Brilliant Blue-stained SDS-PAGE gel containing lysates of AffEpCAM-expressing *L. lactis*. Cont., *L. lactis* containing empty plasmid (pNZ8148); AffEpCAM/IRFP, *L. lactis* expressing EpCAM-targeting affitin and IRFP; flagAffEpCAM/IRFP, *L. lactis* expressing FLAG-tagged EpCAM-targeting affitin and IRFP; IRFP, *L. lactis* expressing infrared fluorescent protein. Arrows denote flagAffEpCAM and AffEpCAM fusion proteins.

Fig. S4. (A–D) Flow cytometry analysis of distribution of *L. lactis* cells displaying the targeting proteins flagAffEpCAM (C) or AffEpCAM (D) to the respective tumor antigen EpCAM, presented by the dot plot display mode of forward scatter (FCS) versus side scatter (SSC). (E–I) Fluorescence of *L. lactis* cells displaying the targeting proteins flagAffEpCAM (G) or AffEpCAM (H), measured in channel FL1. (J) The display of the targeting protein as a shift of the bacteria along the FL1 axis, presented by histogram. Cont. 1, *L. lactis* containing empty plasmid (pNZ8148); Cont. 2, *L. lactis* containing infrared fluorescent protein. Presence of FLAG-tag in the targeting protein is denoted.

Fig. S5. (A–C) Flow cytometry analysis of distribution of *L. lactis* cells displaying the targeting protein Z-HER (C) to the respective tumor antigen HER2, presented by the dot plot display mode of forward scatter (FCS) versus side scatter (SSC). (D-G) Fluorescence of *L. lactis* cells displaying the targeting protein Z-HER (F), measured in channel FL1. (H) The display of the targeting protein as a shift of the bacteria along the FL1 axis, presented by histogram. Cont. 1, *L. lactis* containing empty plasmid (pNZ8148); Cont. 2, *L. lactis* containing infrared fluorescent protein. Presence of FLAG-tag in the targeting protein is denoted.

Fig. S6. (A, B) Western blotting confirmation of expression of EpCAM (A) and HER2 (B) in cell lysates from the HEK293, HT-29, and Caco-2 cells, using the relevant antibodies. (C, D) Representative immunocytochemical staining of transfected HEK293 cells overexpressing fluorescent EpCAM and HER2 using anti-EpCAM (C) and anti-HER2 (D) antibodies. (E, F) Representative immunocytochemical staining of HT-29 (E) and Caco-2 cells (F) using anti-EpCAM and anti-HER2 antibodies (as indicated). Wt, wild-type cells; no plasmid, cells exposed to transfection reagent without plasmid; EpCAM-sfGFP, cells overexpressing EpCAM-sfGFP fusion; HER2-mEm, cells overexpressing HER2-mEmerald fusion; Cont., cells incubated with secondary antibody only; DAPI, DAPI channel; 488, green fluorescence channel; 647, red fluorescence channel.

Fig. S7. Representative imaging flow cytometry analysis of adhesion of EpCAM-targeting (A) and HER2-targeting (C) *L.*

lactis to transfected HEK293 cells, in comparison to *L. lactis* expressing IRFP (control bacteria; B, D). Representative images show HEK293 cells from the upper right quadrant of scatterplots (Fig. 3A, B). The yellow numbers on each image indicate the number of spots, determined using the spot count mask; these spots correspond to *L. lactis* cells. HEK293/EpCAM-sfGFP, HEK293 cells overexpressing sfGFP-labeled EpCAM; HEK293/HER2-mEm, HEK293 cells overexpressing mEmerald-labeled HER2; *L. lactis*/AffEpCAM, *L. lactis* displaying AffEpCAM and expressing IRFP; *L. lactis*/flagZ-HER, *L. lactis* displaying FLAG-labeled Z-HER and expressing IRFP; *L. lactis*/Cont., *L. lactis* expressing IRFP; ChBF, bright-field images; ChG, green fluorescence images (i.e., for tumor antigens); ChR, red fluorescence image (i.e., for *L. lactis*); ChG/ChR, merged green and red fluorescence images.

Fig. S8. Representative imaging flow cytometry analysis of binding of EpCAM-targeting (A) and HER2-targeting (C) *L. lactis* to HEK293 cells in comparison to control *L. lactis* cells (B, D). HEK293/EpCAM-sfGFP, HEK293 cells overexpressing sfGFP-labeled EpCAM; HEK293/HER2-mEm, HEK293 cells overexpressing mEmerald-labeled HER2; *L. lactis*/AffEpCAM, *L. lactis* displaying AffEpCAM and expressing

IRFP; *L. lactis*/flagZ-HER, *L. lactis* displaying FLAG-labeled Z-HER and expressing IRFP; *L. lactis*/Cont., *L. lactis* expressing IRFP; ChBF, bright-field images; ChG, green fluorescence images (i.e., for tumor antigens); ChR, red fluorescence image (i.e., for *L. lactis*); ChG/ChR, merged green and red fluorescence images.

Fig. S9. Representative flow cytometry analysis of adhesion of EpCAM-targeting (A) and HER2-targeting (B) *L. lactis* to transfected HEK293 in comparison with the respective control *L. lactis*. HEK293/EpCAM-sfGFP, HEK293 cells overexpressing sfGFP-labeled EpCAM; HEK293/HER2-mEm, HEK293 cells overexpressing mEmerald-labeled HER2; *L. lactis*/AffEpCAM, *L. lactis* displaying AffEpCAM and expressing IRFP; *L. lactis*/flagZ-HER, *L. lactis* displaying FLAG-labeled Z-HER and expressing IRFP; *L. lactis*/Cont., *L. lactis* expressing IRFP.

Fig. S10. Linear regression for the number of *L. lactis* cells associated with each tumor cell determined by manual counting and ImageJ counting for the HT-29 (A) and Caco-2 (B) cells. Below: R^2. AffEpCAM/IRFP, *L. lactis* displaying AffEpCAM and expressing IRFP; flagZ-Her/IRFP, *L. lactis* displaying FLAG-labeled Z-HER and expressing IRFP.